Available online www.jsaer.com

***Journal of Scientific and Engineering Research*, 2023, 10(2):163-172**

Research Article

ISSN: 2394-2630
CODEN(USA): JSERBR

Prediction of forming limit of dual phase steel DP780 at 673k temperature based on GTN model

Xingfeng Liu, Di Li*, Hui Song, Zipeng Lu, Hongjian Cui

School of Traffic and Vehicle Engineering, Shandong University of Technology, Zibo, China

Abstract The GTN damage parameters of DP780 steel at 673k temperature were determined by experimental method and finite element back calibration method. In order to obtain the forming limit curve and the value of FLC_0, the DP780 steel with different thickness at 673k temperature was numerically simulated and verified by a few experiments. The calculation formulas of forming limit curve and FLC_0 are given, which are verified by tensile bending samples. The results show that the 673K temperature forming limit curve of DP780 obtained by numerical simulation based on GTN damage model can accurately predict the forming of DP780 sheet at 673K temperature.

Keywords Advanced high strength dual-phase steel, DP780, Warm forming, forming limit, GTN model

1. Introduction

With the development of automobile lightweight technologies, the application of warm forming process is more and more extensive. It is now one of the main development directions of plastic forming. By employing the warm forming process, the strength and plasticity advantages of dual-phase steel can be better utilized.

The Gurson-Tvergaard-Needleman (GTN) model (Gurson A. L., 1997) is an important tool for studying meso-damage theory. Gholipour, H (2019) et al. determined the void-related parameters in the GTN model through the uniaxial tensile test of low carbon steel, and determined the spherical fracture mechanism under different stress conditions. Li X (2020) et al. studied the effect of damage evolution of GTN model on plastic deformation under different stress triaxiality. GTN model is also widely used to predict the forming limit of sheet metal and judge the fracture position in the process of sheet metal forming (Zao H. A. et al, 2020; Liu, W. Q. et al, 2018; Cui, X. L. et al, 2018). Most researchers use the combination of numerical simulation and experiment to determine the damage parameters of GTN model, and further realize the prediction of sheet metal forming through numerical simulation. Oh, C. K. (2007) et al. proposed the method of combining single tensile test curve with finite element to obtain the meso damage parameters of GTN. Sun, Q. (2020) et al. determined the material parameters of the shear modified GTN damage model through small punch test and numerical simulation. Safdarian, R. et al. (2018) obtained the forming limit curve of AA6016-T4 sheet based on the GTN damage model by writing the VUMAT subroutine simulation, and verified that the GTN model is an effective tool for analyzing the formability of anisotropic sheet metal. Huang, T. (2019) et al. determined the parameters in the GTN model through the finite element reverse method, and used the plastic constitutive formula derived from the GTN model to obtain the forming limit diagram under plastic conditions. Kami, A. et al. (2015) quickly determined the GTN model parameters of AA6016-T4 aluminum alloy based on the response surface method and the numerical simulation results of uniaxial tensile test.

The GTN damage model is widely used in the material forming process, but there are few studies and applications for the material in the warm forming process. Warm forming has great advantages over cold and hot stamping, and is now one of the main development directions of plastic forming. Carsley, P. J. et al. (2006) designed the UMAT subroutine and carried out simulation analysis using GTN model at many different temperatures. Henseler, T. (2020) studied the GTN model material parameters of AZ31 magnesium flakes at different temperatures. Zhao, P. J. (2016) et al. conducted a joint experimental-numerical study of the failure of AZ31Mg alloy sheets during hot stamping based on a modified GTN-damage model incorporating the Yid 2000 anisotropic yield criterion. When studying the warm forming process of DP780 dual phase steel, some scholars found that the sheet metal forming was better at 673k (Wang Kaidi et al, 2021; Han Meng et al, 2021; Liu Dahai et al, 2017).

In this paper, the numerical simulation of hemispherical punching tensile test based on GTN model is carried out by using ABAQUS explicit user material subroutine. The damage parameters of DP780 dual phase steel at 673k temperature were determined by uniaxial tensile test and numerical simulation. The stress and strain are obtained at the last loading step before crack. The forming limit curves of DP780 dual phase steel with different thickness at 673k temperature are drawn and verified by a small number of tests. Finally, the forming limit curve formula is fitted, and the relationship between FLC_0 and sheet thickness is obtained, which is verified by tension bending specimens. It is confirmed that the GTN model parameters determined by finite element inverse standard can be used to study the forming limit of ductile metal, which provides theoretical basis and technical guidance for production.

2. GTN damage model

The GTN damage model is a commonly used constitutive model for mesoscopic damage analysis of materials. The GTN damage model is shown in Eq. (2.1):

$$\Phi = \left(\frac{q}{\sigma_m}\right)^2 + 2q_1 f^* \cosh\left(\frac{3q_2\sigma_h}{2\sigma_m}\right) - \left(1 + q_3 f^{*2}\right) \tag{2.1}$$

Where q is the Mises equivalent stress, σ_h is the hydrostatic pressure, σ_m is the equivalent stress of the material, q_1, q_2, q_3 is the strengthening parameter, f^* is the void volume fraction function and:

$$f^* = \begin{cases} f & f \le f_c \\ f_c + \delta(f - f_c) & f > f_c \end{cases} \tag{2.2}$$

$$\delta = \frac{f_u^* - f_c}{f_f - f_c} \tag{2.3}$$

Where f_c is the critical pore volume fraction when the pores begin to polymerize, f_f is the pore volume fraction when the material ruptures, δ is the pore growth acceleration factor, f_u^* is the f^* value when the stress in the yield equation is 0.

The growth of void volume fraction is divided into two parts: the growth of original void and the nucleation of new void:

$$\dot{f} = f_g + f_n \tag{2.4}$$

Since the material is assumed to be incompressible, according to the law of conservation of mass, the change of void volume fraction caused by void growth is only related to hydrostatic stress (Marouani, H. et al, 2009):

$$f_g = (1 - f)\, d\varepsilon^p : I \tag{2.5}$$

Where ε^p is the plastic strain tensor, I is the second-order unit tensor.

The nucleation criterion adopted in this paper is controlled by plastic strain. The change of void volume fraction caused by void nucleation is expressed by the following formula:

$$f_n = \frac{f_N}{s_N\sqrt{2\pi}}\exp\left[-\frac{1}{2}\left(\frac{\varepsilon_m^{pl}-\varepsilon_N}{s_N}\right)^2\right]\dot{\varepsilon}_m^{pl} \tag{2.6}$$

Where f_N is the void volume fraction of nucleatable particles, s_N is the average strain during hole nucleation, ε_N is the standard deviation of strain, $\dot{\varepsilon}_m^{pl}$ is the growth rate of plastic volumetric strain, ε_m^{pl} Is the equivalent plastic strain of the matrix.

3. GTN model parameter calibration

3.1 Material performance parameters

Before applying the GTN damage model to predict the damage of the DP780 sheet, the 12 undetermined parameters in the model need to be calibrated. Mainly hardening parameters $K, \varepsilon_0, \mathrm{n}$, nucleation related parameters ε_N, s_N, f_N, hole parameters f_0, f_c, f_f and strengthening parameters q_1, q_2, q_3. In order to determine these parameters, according to the national standard GB/T4338-2006 "Metallic Material High Temperature Tensile Test Method", a uniaxial tensile test at 673K was carried out on DP780 steel plate with a thickness of 1mm. The tensile specimen is cut from DP780 plate along the rolling direction (RD), 45°direction and transverse (TD). The test was carried out on the WDW-20D universal testing machine, and the tensile speed was set to 0.2mm/min at 673K. Before the tensile test, the DP780 sample was heated to 673k. The temperature of the specimen remains stable until the specimen is stretched to a crack. To ensure the accuracy of the results, the same three sets of specimens were subjected to uniaxial tensile tests to take the average value. The dimensions are shown in Fig.1. Table 1 summarizes the chemical composition of the DP780.

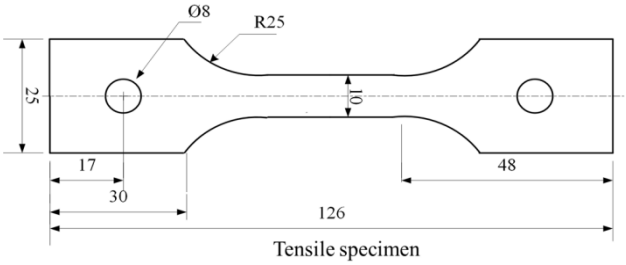

Figure 1: Dimension diagram of the tensile specimen

Table 1: The chemical composition of DP780 and its mass fraction%

C	Si	Mn	P	S	Al
0.1	0.16	2.02	0.08	0.03	0.039

The sample result diagram obtained through the above test and the extracted engineering and actual stress-strain diagram are shown in Fig.2.a and b. In order to determine the mechanical properties and hardening behavior of DP780 sheet at 673k, the famous swift law has been applied.

$$\sigma = \mathrm{k}\left(\varepsilon_0 + \bar{\varepsilon}_\mathrm{p}\right) \tag{3.1}$$

Where ε_0 $\bar{\varepsilon}_\mathrm{p}$ and n are the material hardening constant is determined by extrapolation of the experimental stress-strain curve using the least square method (Fig.2.C). The quantities identified for the material elastic-plastic parameters are listed in the Table 2.

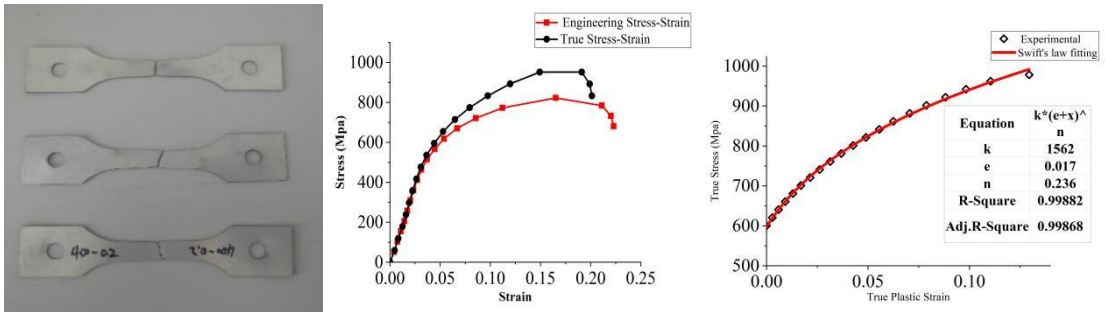

(a) (b) (c)

Figure 2: (a) Specimen drawing and (b) engineering and true stress-strain plots and (c)true plastic stress-strain approximate curve for realizing hardening parameters

Table 2: Elastoplastic material parameters of DP780 steel plate

E(Mpa)	v	k(Mpa)	ε_0	n
185000	0.31	1562	0.017	0.236

3.2 Damage parameters

The damage parameters mainly affects the plastic deformation process of the material. Tvergaar (1984) considered the strength loss caused by the interaction of pores, the influence of the stress triaxiality and the pore volume fraction, and introduced three constants q_1, q_2, q_3 as the strengthening parameters. In order to better understand the quantitative range of GTN model parameters of different materials,through research literature, as shown in the following Table 3:

Table 3: The GTN model parameters in the reference

Author	Material	q_1	q_2	q_3	ε_N	s_N	f_N	f_0	f_c	f_f
Schmitt, W. (1997) et al.	20MnMoNi55	1.5	1	2.25	0.3	0.1	0.002	0	0.06	0.212
Ridha, Hambli. (2001) et al.	Carbon steel	1.5	1	2.25	0.3	0.1	0.04	-	-	-
Achouri, M. (2013) et al.	HSLA	1.5	1	2.25	0.3	0.1	0.02	0.0015	0.08	0.13
Springmann, M. (2005) et al.	Carbon steel	1.5	1	2.25	0.3	0.1	0.01	0.001	0.01	0.15
Kiran, R. (2014) et al.	ASTM A992	1.5	1	2.25	0.2	0.1	0.02	0	0.03	0.5

According to the literature research results, this paper selects q_1=1. 5, q_2=1, q_3 = 2.25

Other damage parameters are generally determined by direct and indirect methods. In order to improve the accuracy of determining the parameters. In this paper, the finite element method and RSM experimental design are used to determine the value of damage parameters. Due to the excessive number of parameters, in order to accurately conduct the research, it was decided to reduce the number of parameters to be determined. The ε_N, s_N values of 0.3 and 0.1 were determined through the above literature data, and the remaining four parameters were selected for research (Table 4).

Table 4: Range of values of damage parameters

Parameter	f_N	f_0	f_c	f_f
Select range	0.021-0.06	0.002-0.005	0.018-0.052	0.036-0.1

The remaining four parameters are calibrated using the RSM reverse analysis method based on the central composite design (CCD). The GTN damage model is used to describe the constitutive relationship of the material, and the predicted curve is consistent with the test curve, and the appropriate value of damage parameters can be found. In order to obtain a good prediction effect, the displacement under peak maximum

force (R_1) and peak maximum force (R_2) are selected as the response target. In addition, this paper chooses a quadratic polynomial regression model to fit the functional relationship between the response variable and the four influencing parameters, as shown in the formula:

$$Y = b_0 + \sum_{i=1}^{4} b_i x_i + \sum_{i=1}^{4} b_{ii} x_i^{\,2} + \sum_{i=1}^{3} \sum_{j=i+1}^{4} b_{ij} x_i x_j \tag{3.2}$$

According to the experimental design (Table 5), each group is numerically simulated to obtain different response values.

Table 5: Design scheme of damage parameters and response values

Run	f_N	f_0	f_c	f_f	Run	f_N	f_0	f_c	f_f
1	0.021	0.002	0.052	0.1	15	0.06	0.002	0.052	0.1
2	0.06	0.002	0.018	0.036	16	0.06	0.005	0.052	0.1
3	0.0405	0.0035	0.035	0.068	17	0.021	0.005	0.052	0.036
4	0.06	0.002	0.018	0.1	18	0.06	0.005	0.018	0.036
5	0.06	0.002	0.052	0.036	19	0.0405	0.0035	0.001	0.068
6	0.06	0.005	0.018	0.1	20	0.0405	0.0065	0.035	0.068
7	0.021	0.002	0.018	0.036	21	0.0405	0.0005	0.035	0.068
8	0.021	0.005	0.052	0.1	22	0.0405	0.0035	0.035	0.132
9	0.06	0.005	0.052	0.036	23	0.0405	0.0035	0.035	0.068
10	0.021	0.005	0.018	0.1	24	0.0405	0.0035	0.035	0.004
11	0.0405	0.0035	0.035	0.068	25	0.0795	0.0035	0.035	0.068
12	0.021	0.002	0.018	0.1	26	0.0015	0.0035	0.035	0.068
13	0.021	0.005	0.018	0.036	27	0.0405	0.0035	0.035	0.068
14	0.021	0.002	0.052	0.036	28	0.0405	0.0035	0.069	0.068

The ANOVA method is used to evaluate the established quadratic polynomial regression model, and the analysis and summary are shown in the Table 6.

Table 6: ANVOA analysis

Response	R_1	R_2
Regression P value	0.00002	0.0001
R^2 %	93.06	92.38

All regression P values are less than 0.01, indicating that the model is statistically significant, the values of R^2 are all higher than 90%, indicating that the model has a good level of regression. By analyzing the significance of the regression coefficients, a quadratic polynomial regression equation is established:

$$\begin{aligned} R_1 = {} & 707.35 - 11.46 f_n + 7.22 f_0 + 27.99 f_c + 4.85 f_f - 22.05 f_n f_0 - 2.96 f_n f_c - 2.94 f_n f_f \\ & + 12.86 f_0 f_c - 2.81 f_0 f_f + 1.14 f_c f_f + 42.70 f_n^{\,2} - 10.73 f_0^{\,2} 14.61 f_c^{\,2} - 7.60 f_f^{\,2} \end{aligned} \tag{3.3}$$

$$\begin{aligned} R_2 = {} & 0.275 - 0.0224 f_n + 0.0482 f_0 + 0.0623 f_c + 0.0709 f_f - 0.0709 f_n f_0 - 0.0252 f_n f_c - 0.0048 f_n f_f \\ & + 0.0446 f_0 f_c - 0.0058 f_0 f_f + 0.002 f_c f_f + 0.1512 f_n^{\,2} - 0.0236 f_0^{\,2} - 0.026 f_c^{\,2} - 0.0194 f_f^{\,2} \end{aligned} \tag{3.4}$$

In order to solve the above regression equation, through MATLAB genetic algorithm, the appropriate damage parameters of DP780 steel at 673K are finally determined (Table 7).

Table 7: Damage parameter values

temperature	f_N	f_0	f_c	f_f
673K	0.036	0.004	0.026	0.065

The curve obtained by numerical simulation using the appropriate damage parameters obtained above is compared with the test curve (Fig.3). The maximum error is 5.2%, indicating that the damage parameters calibrated by the finite element method are accurate.

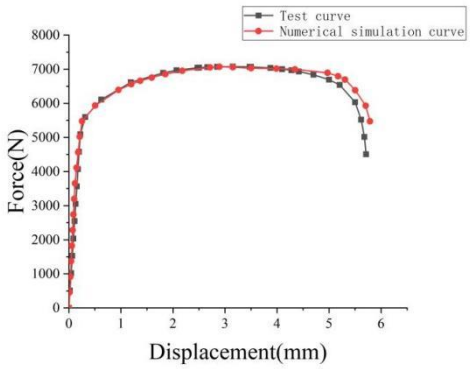

Figure 3: Comparison between simulated force-displacement curve and experimental force-displacement curve at 673k

4. FLC curve at 673K

In order to predict and verify the forming limit, the finite element models of expansion test and tensile bending test are established. Through the damage parameters calibrated in the previous section, the VUMAT subroutine considering GTN damage is embedded into ABAQUS for numerical simulation.

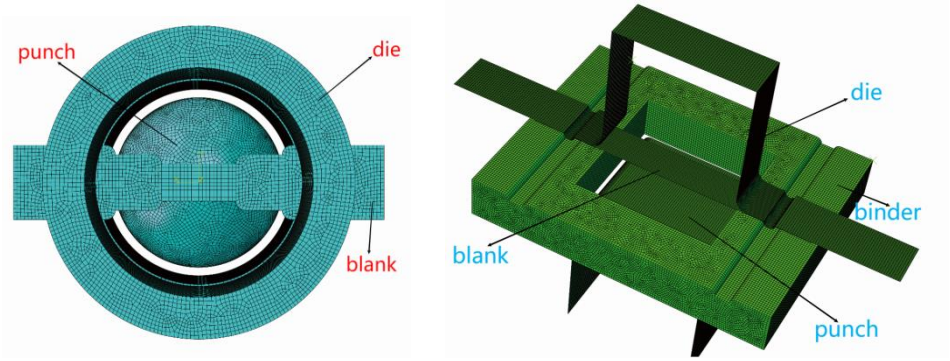

(a) (b)

Figure 4: (a) Drawing of bulging die and sample and (b) Drawing of tensile bending test mould and sample

4.1 Numerical Simulation

In order to determine the forming limit curve of DP780 dual phase steel with different thickness under 673k condition according to GTN damage model, numerical simulation tests were carried out on samples with thickness of 0.8mm, 1.0mm, 1.2mm, 1.6mm and 2.0mm respectively according to the above determined GTN damage model parameters. The numerical simulation results are shown in the figure below (taking 1mm as an example).

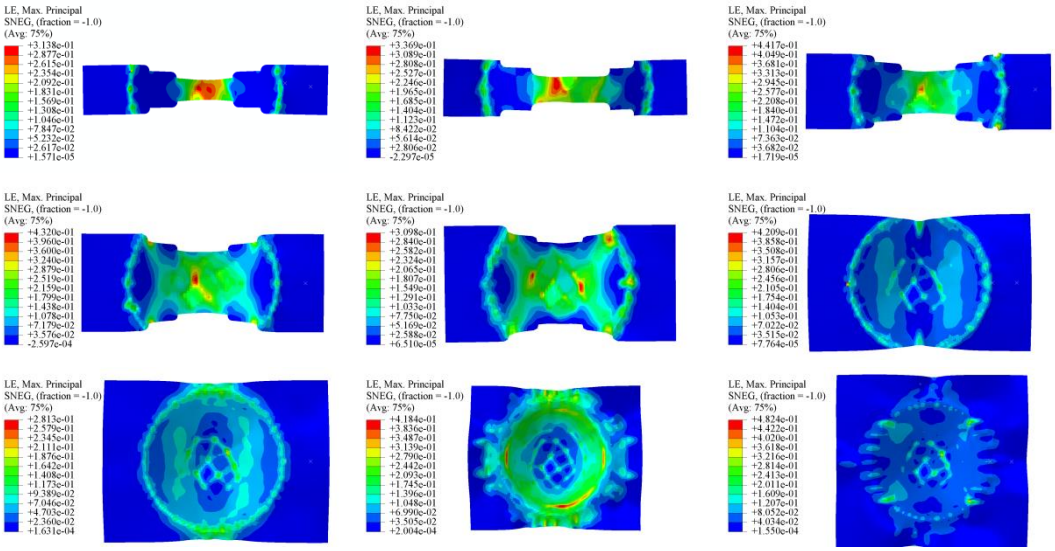

Figure 5: Numerical simulation diagram of principal strain in bulging test

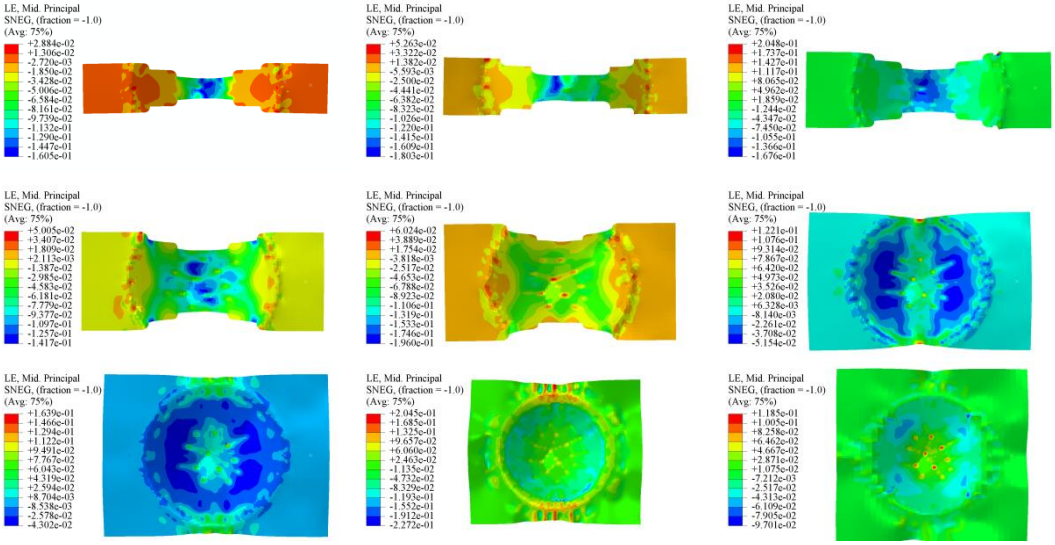

Figure 6: Numerical simulation diagram of secondary strain in bulging test

Extract the ultimate primary and secondary strains when the sample is broken in the simulation, draw the FLC curve according to the ultimate maximum primary strain and secondary strain, and obtain the 0.8mm, 1.0mm, 1.2mm, 1.6mm and 2.0mm DP780 steel forming limit curve and FLC_0 values at different thicknesses.

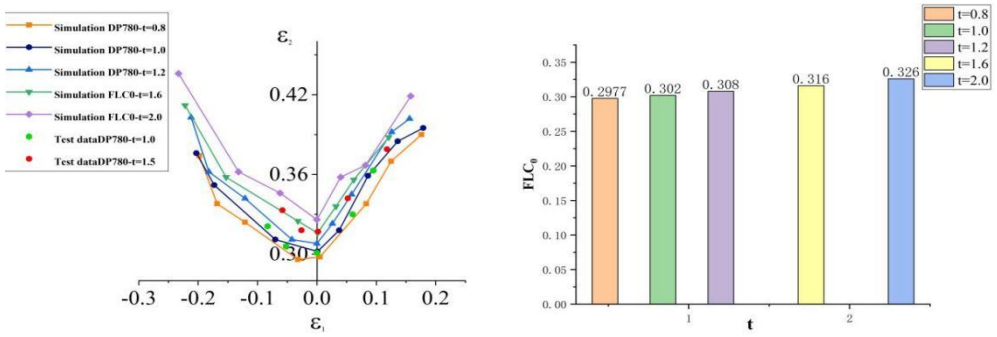

Figure 7: Forming limit curve and FLC_0 value of DP780 sheet with different thickness at 673k

Passing the partial bulge test with a thickness of 1mm and 1.5mm, the primary and secondary strains of the measured specimen are compared with the numerical simulation results (Fig.7), and the maximum error is found to be 5.63%. It shows that the forming limit curve of 673K DP780 dual-phase steel obtained by numerical simulation can be used for fracture failure prediction.

In order to make the application of forming limit curve more convenient, according to the numerical simulation results, the 673K forming calculation model of DP780 dual-phase steel is established, that is, it is assumed that the left tension-compression zone of the forming limit curve is a straight line, and the right tension-tension zone is an exponential growth mode. The mathematical expression is as follows:

$$\begin{cases} \varepsilon_1 = 0.302 - 0.358\varepsilon_2, \varepsilon_2 < 0 \\ \varepsilon_1 = 0.302 + 0.054e^{-5.56\varepsilon_2}, \varepsilon_2 \geq 0 \end{cases} \quad (4.1)$$

Where ε_1 is the principal strain, ε_2 is the secondary strain.

FLC_0 is the limit strain point of the forming limit diagram curve. The stress state under the strain path corresponding to the ultimate strain point is a pure shear state. Through Zhu Hongchuan, (2017) et al. It is known that FLC_0 is suitable for the judgment of sheet metal forming under 2mm. According to the above numerical simulation, the relationship between the FLC_0 point and the hardening index n of the DP780 sheet with different thicknesses is determined.

$$FLC_0 = 2.782n + 0.04t - 0.187 \qquad t \leq 2mm \quad (4.2)$$

4.3. Forming limit curve application

At the temperature of 673k, using the FLC curve obtained in the previous section, the tensile bending simulation with punching fillet radius of 5mm and bending depth of 15.5mm was carried out (Fig.4.(b)), and the corresponding tests were carried out. The example results are shown in Fig. 8.

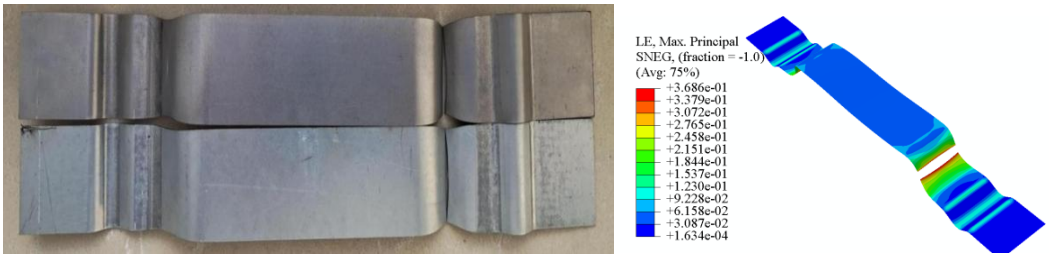

Figure 8: Tensile bending test results and numerical simulation results

Through the test, it can be seen that the specimen with a tensile-bending depth of 15.5mm appears to be broken, the broken position is off-rounded to the lower side wall, and a certain degree of necking occurs, which is consistent with the numerical simulation results. Therefore, the formation limit curve of DP780 at 673k simulated by the GTN damage parameters inversely calibrated by finite element can accurately predict the formation of DP780.

5. Conclusion

In this paper, the mechanical property parameters of DP780 dual phase steel and the damage parameters of GTN model at 673k are calibrated by RSM experimental design, unidirectional tensile test and numerical simulation. Using the GTN damage model parameters obtained by finite element back calibration as the failure criterion, the forming limit curves of DP780 dual phase steel with different thickness at 673k temperature are drawn and verified by a small number of tests. The relationship between flc0 and thickness and the prediction equation of FLC curve are established. Finally, through the tensile bending test, it is

verified that the damage parameters of the finite element inverse standard GTN model can be used to study the forming limit of DP780 at 673k.The main conclusions of this research are:

The hardening coefficient K and hardening exponent n of DP780 steel at 673K were determined by uniaxial tensile test of DP780 dual-phase steel. The damage parameters of the GTN model were determined by the response surface method (RSM). The damage parameters of the GTN model f_c, f_f, f_0, f_N at 673K were 0.082, 0.176, 0.0016, and 0.03, respectively. The numerical simulation is compared with the experimental results, and it is found that the calibrated parameters have good applicability.

(2) The finite element simulation software ABAQUS was used to embed the VUMAT subroutine based on the GTN damage criterion to carry out the numerical simulation of the bulging test at 673K. For verification, the maximum error is 5.63%, which indicates that the forming limit model considering GTN damage is suitable. Through numerical simulation and data processing under different thicknesses, the formula of forming limit curve is fitted, and the determination method of FLC_0 is given. It is verified that the damage parameters of the finite element inverse standard GTN model can be used to study the forming limit of DP780 at 673k, which provides a reference for the warm stamping process of DP780 dual phase steel.

References

[1]. Gurson A. L., 1977, Continuum theory of ductile rupture by void nucleation and growth: part i—yield criteria and flow rules for porous ductile media, Journal of Engineering Materials and Technology, 99(1), 297-300

[2]. Gholipour, H., Biglari, F. R., Nikbin, K., 2019, Experimental and numerical investigation of ductile fracture using gtn damage model on in-situ tensile tests, International Journal of Mechanical Sciences, 164, 105170

[3]. Li X., Chen Z., Dong C., 2020.,Size effect on the damage evolution of a modified gtn model under high/low stress triaxiality in meso-scaled plastic deformation, Materials Today Communications, 101782

[4]. Zao H. A., Hao Z., Yh A., 2020, An improved shear modified gtn model for ductile fracture of aluminium alloys under different stress states and its parameters identification - sciencedirect, International Journal of Mechanical Sciences, 192

[5]. Liu, W. Q., Ying, L., Dai, M. H., Hu, P., Wang, D. T., 2018, Parameter calibration for a shear modified gtn model and its application to forming limit prediction, Journal of Physics Conference, 1063

[6]. Cui, X. L., Zhang, W. W., Zhang, Z. C. , Chen, Y. Z., Peng, L., Chi, C. Z., 2018, Prediction of forming limit of dual-phase 500 steel sheets using the gtn ductile damage model in an innovative hydraulic bulging test, JOM: the journal of the Minerals, Metals & Materials Society, 70, 1542–1547

[7]. Oh, C. K., Kim, Y. J., Baek, J. H., Kim, Y. P., Kim, W., 2007, A phenomenological model of ductile fracture for api x65 steel,International Journal of Mechanical Sciences, 49(12), 1399-1412

[8]. Sun, Q., Lu, Y., Chen, J., Sun, Q., Chen, J., 2020, Identification of material parameters of a shear modified gtn damage model by small punch test,International Journal of Fracture

[9]. Safdarian, R., 2018, Forming limit diagram prediction of 6061 aluminum by gtn damage model,Mechanics and Industry, 19(2)

[10]. Huang, T., Zhan, M., Wang, K., Chen, F., Bai, L., 2019, Forming limit stress diagram prediction of pure titanium sheet based on gtn model, Materials, 12(11), 1783

[11]. Kami, A., Dariani, B. M., Vanini, A. S., Comsa, D. S., D Banabic., 2014, Numerical determination of the forming limit curves of anisotropic sheet metals using gtn damage model, Journal of Materials Processing Technology, 216, 472-483

[12]. Carsley, P. J., 2006, Forming of aluminum alloys at elevated temperatures -part 2: numerical modeling and experimental verification, International Journal of Plasticity

[13]. Henseler,T., 2020, GTN Model-Based Material Parameters of AZ31 Magnesium Sheet at Various Temperatures by Means of SEM, In-Situ Testing CRYSTALS, 10(10), 2073-4352
[14]. Zhao, P. J., Chen, Z. H., Dong, C. F., 2016, Experimental and numerical analysis of micromechanical damage for dp600 steel in fine-blanking process, Journal of Materials Processing Tech, 236, 16-25
[15]. Wang Kaidi, Li Di, Leng Yangsong, Fu Qiutao, Xu Jiachuan, Jiang Ning, 2021, Study on warm forming limit prediction of advanced high strength steel DP780 sheet metal(in Chinese), Mechanical strength, 05, 1177-1183
[16]. Han Meng, Li Di, Wang Kaidi, Xu Jiachuan, Jiang Ning, 2021, Determination of meso damage parameters and temperature dependent law of high strength dual phase steel DP780(in Chinese), 05, Journal of Applied Mechanics, 2064-2068
[17]. Liu Dahai, Xu gangbi, Chang Chun, 2017, DP780 high strength steel sheet warm forming limit diagram and its calculation model(in Chinese), Journal of plastic engineering, 02, 192-197
[18]. Marouani, H., Ismail, A. B., Hug, E., Rachik, M., 2009, Numerical investigations on sheet metal blanking with high speed deformation, Materials & Design, 30(9), 3566-3571.
[19]. Tvergaard, V., N Ee Dleman, A., 1984, Analysis of the cup-cone fracture in a round tensile bar, Acta Metallurgica, 32(1), 157-169
[20]. Schmitt, W., Sun, D. Z., Blauel, J. G., 1997, Damage mechanics analysis (gurson model) and experimental verification of the behaviour of a crack in a weld-cladded component, Nuclear Engineering & Design, 174(3), 237-246
[21]. Ridha, Hambli., 2001, Comparison between lemaitre and gurson damage models in crack growth simulation during blanking process, International Journal of Mechanical Sciences, 43(12), 2769-2790
[22]. Achouri, M., Germain, G., Santo, P. D., Saidane, D., 2013, Numerical integration of an advanced gurson model for shear loading: application to the blanking process, Computational Materials Science, 72, 62–67
[23]. Springmann, M., Kuna, M., 2005, "identification of material parameters of the gurson–tvergaard–needleman model by combined experimental and numerical techniques" , Computational Materials Science, 33(4), 500-500
[24]. Kiran, R., Khandelwal, K., 2014, Gurson model parameters for ductile fracture simulation in astm a992 steels, Fatigue & Fracture of Engineering Materials and Structures
[25]. Zhu Hongchuan, Wang Youlu, Wei Xing, Yang Bing, 2017, Calculation of forming limit curve of high strength low alloy steel (in chinese), Iron and Steel Research, 06, 63-66